Direct Tunneling and Gate Current Fluctuations

O. Baumgartner*, M. Bina*, W. Goes*, F. Schanovsky*, M. Toledano-Luque†, B. Kaczer†, H. Kosina*, T. Grasser*
*Institute for Microelectronics, TU Wien, Gußhausstraße 27–29, 1040 Wien, Austria
Email: {baumgartner|bina|goes|schanovsky|kosina|grasser}@iue.tuwien.ac.at
†imec, Kapeldreef 78, B-3001 Leuven, Belgium
Email: {toleda|kaczer}@imec.be

***Abstract*—A comprehensive study of correlated gate leakage and drain current fluctuations in nMOS devices using non-equilibrium Green's function calculations has been carried out. A simulation model combining 3D self-consistent electrostatic potentials accounting for random discrete dopants and charged oxide traps with a 1D and 2D transport description of direct-tunneling gate leakage has been developed. The influence of the charge state of the trap on the direct-tunneling current has been investigated. A considerable local change in current density around the trap has been observed. By varying the position of the trap it has been found that oxide defects close to the drain and source regions have a higher impact on the gate leakage. A statistical analysis of nMOSFETs by varying the configuration of the random discrete dopants has been performed. The trap has been positioned close to the drain to achieve a worst-case scenario. The reduction in direct-tunneling current due to charging of a single trap has been calculated for each device. Gate current reductions below one percent have been found. The experimentally measured large gate leakage fluctuations can thus not be accounted for with direct tunneling.**

I. Introduction

Due to the continuing miniaturization of metal-oxide-semiconductor (MOS) devices, fluctuations in the drain current increasingly affect the device operation [1]. This so-called random telegraph noise (RTN) has been well studied and is now understood to consist of charge capture and emission events into and out of oxide defects. It has been recently reported in [2], [3], [4] that the fluctuations of the drain and the gate current can be correlated. Quite remarkably, the relative drop in gate current can reach up to 80 % (Fig. 1) and is independent of temperature [2]. Microscopically this means that the magnitude of the gate current is linked to the charge state of the oxide defects.

In this work we investigate direct tunneling as possible physical cause of the gate RTN in nMOS transistors. The direct tunneling current is reduced by charged oxide defects through a changed electrostatic configuration. An alternative explanation relies on the multi-state defect model [5], in which the gate leakage current is described by trap-assisted tunneling (TAT). Fig. 2 shows schematically how the direct-tunneling current and the trap-assisted tunneling current are influenced by a charged trap.

II. Simulation Method

To calculate the direct-tunneling gate leakage, we used the non-equilibrium Green's function (NEGF) models that are part of our quantum simulation framework Vienna Schrödinger-Poisson (VSP) [6].

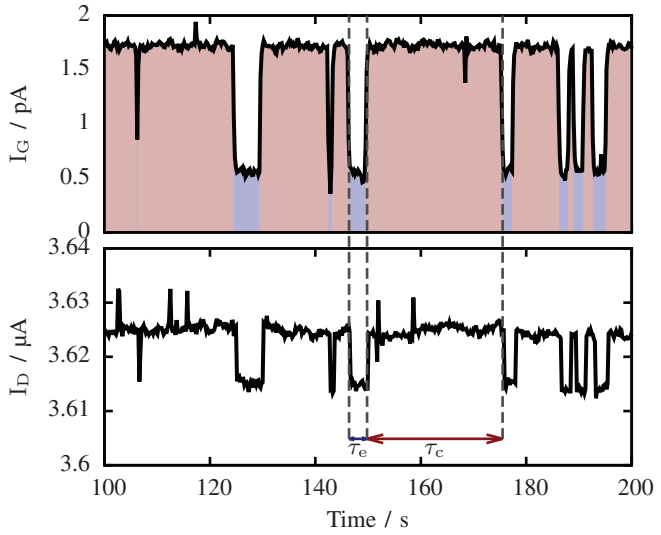

Fig. 1. Simultaneously recorded traces of gate (bottom) and drain (top) current in an nMOSFET with effective oxide thickness of 2.3 nm [2]. After an electron is captured, the charged trap reduces I_D. Concurrently, the gate current decreases significantly. After the electron is emitted (τ_e), the currents return to normal levels. Similar relative drops in gate current have been observed for varying temperature (cf. [2]).

The retarded and advanced Green's functions are determined by the equation

$$G^{\mathrm{R}}(\mathbf{r},\mathbf{r}',\mathcal{E}) = G^{\mathrm{A}\dagger}(\mathbf{r},\mathbf{r}',\mathcal{E}) = [\mathcal{E}I - H(\mathbf{r},\mathbf{r}',\mathcal{E}) - \Sigma^{\mathrm{R}}(\mathbf{r},\mathbf{r}',\mathcal{E})]^{-1}, \quad (1)$$

where $H(\mathbf{r},\mathbf{r}',\mathcal{E})$ is the Hamiltonian of the system. $\Sigma^{\mathrm{R}}(\mathbf{r},\mathbf{r}',\mathcal{E})$ is the retarded self-energy that contains the description of the semi-infinite lead regions. The lesser Green's function is calculated as

$$G^{<}(\mathbf{r},\mathbf{r}',\mathcal{E}) = G^{\mathrm{R}}(\mathbf{r},\mathbf{r}',\mathcal{E})\Sigma^{<}(\mathbf{r},\mathbf{r}',\mathcal{E})G^{\mathrm{A}}(\mathbf{r},\mathbf{r}',\mathcal{E}). \quad (2)$$

The lesser self energy of the left and right contact is given by $\Sigma^{<}_{\mathrm{l,r}}(\mathcal{E}) = \mathrm{i}\Im\{\Sigma^{\mathrm{R}}_{\mathrm{l,r}}(\mathcal{E})\}f_{\mathrm{l,r}}(\mathcal{E})$ with the occupation function $f_{\mathrm{l,r}}(\mathcal{E})$ of the left and right lead, respectively. The Green's functions allow the calculation of physical quantities of interest such as the local density of states, $N(\mathbf{r},\mathbf{r},\mathcal{E}) = -\frac{1}{\pi}\Im\{G^{\mathrm{R}}(\mathbf{r},\mathbf{r},\mathcal{E})\}$, and the electron and current density

$$n(\mathbf{r}) = -2\mathrm{i}\int G^{<}(\mathbf{r},\mathbf{r},\mathcal{E})\frac{d\mathcal{E}}{2\pi}, \quad (3)$$

$$j(\mathbf{r}) = -\frac{\hbar q}{m^*}\int \left[(\nabla - \nabla')G^{<}(\mathbf{r},\mathbf{r}',\mathcal{E})\right]\Big|_{\mathbf{r}'=\mathbf{r}}\frac{d\mathcal{E}}{2\pi}. \quad (4)$$

978-1-4673-5736-4/13/$31.00 ©2013 IEEE

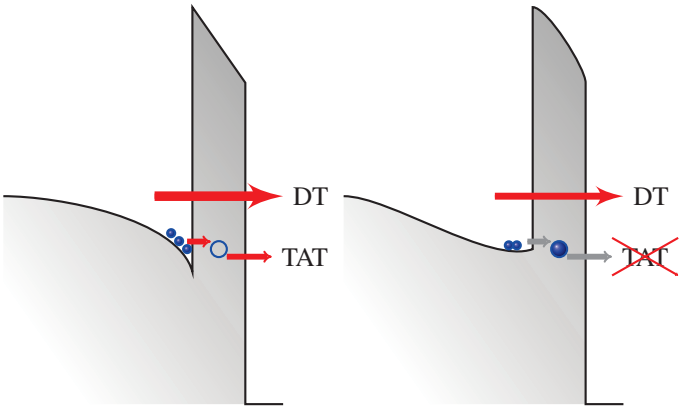

Fig. 2. Principal contributions to gate leakage current; left: an inactive trap can contribute to the gate leakage through trap-assisted tunneling; right: the occupied trap prevents trap-assisted tunneling. Through changed electrostatics the carriers are pushed away from the interface and the oxide barrier shape changes; The influence of this effect on the direct-tunneling current and eventually the gate leakage is the topic of this paper.

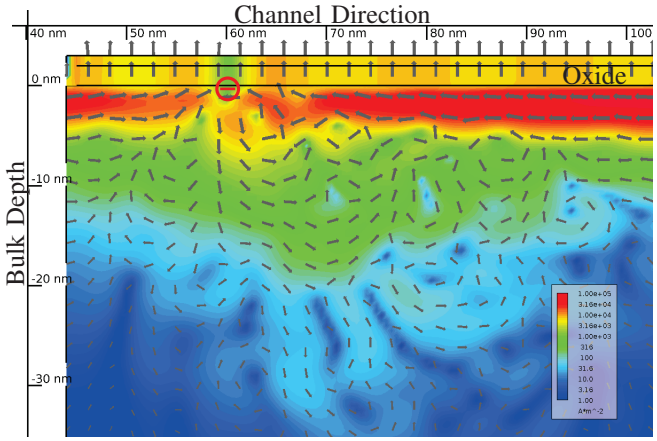

Fig. 3. Current density calculated using the 2D NEGF model. The current in the channel flows around the charged defect at 60 nm. The tunneling current at the defect is significantly reduced. Furthermore, the current vectors show that the gate leakage current through the oxide flows perpendicular to the interface. Therefore, a 1D model is capable of describing the direct-tunneling transport through the oxide correctly.

The numerical evaluation of the carrier concentration and the current requires a discretization of the energy space. It is essential to correctly resolve narrow resonances while keeping the number of energy grid points low to prevent an unpredictable summation of numerical errors and intractable memory requirements. Adaptive energy integration (AEI) on a non-equidistant grid is required to increase accuracy, numerical stability, and memory efficiency. The different approaches that were implemented and tested for applicability to the NEGF formalism are outlined in [7].

For 1D transport we implemented a decoupled multi-valley effective mass NEGF model [8] based on the recursive Green's function method presented in [9]. For 2D quantum transport simulations an NEGF model based on the formalism from [10] has been realized.

As input for the quantum transport simulations we used

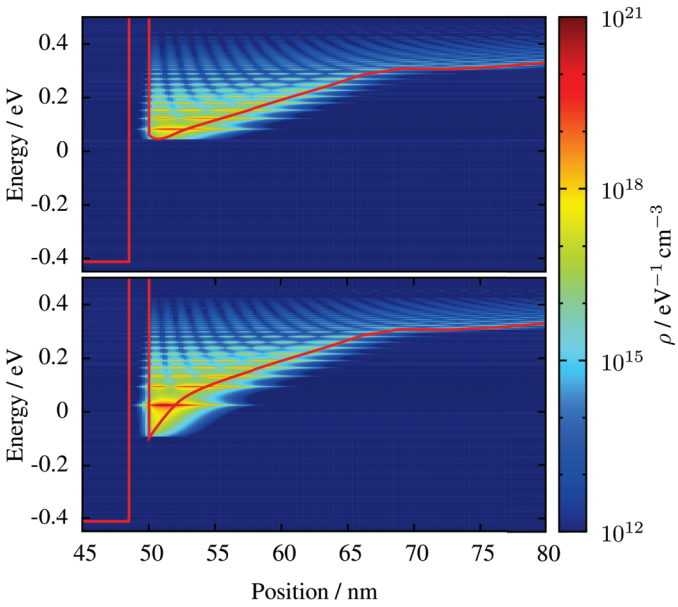

Fig. 4. Local density of carriers for the nMOSFET with inactive trap (bottom) and charged trap (top). The local effect of the charged trap on the carriers is clearly visible. The wave functions are pushed away from the interface. Consequently, the current density is affected by the change in carrier concentration.

cuts on the 3D electrostatic potential calculated by MinimosNT. For the 1D model we cut perpendicularly to the gate oxide and for the 2D model the cut plane goes along the channel from source to drain. The electrostatic potential was interpolated on the new grid for the transport calculation. For these potential profiles we then calculated the tunneling current using NEGF.

III. Direct Tunneling and Defects

The magnitude of the direct-tunneling current through the gate is determined by the shape of the wavefunction in the inversion layer. One can argue that the charge captured by the defect locally repels the inversion charge resulting in a shift of the wavefunction away from the interface and thus in a reduced tunneling current.

As test devices we modeled nMOSFETs with a gate area of 65×65 nm^2, an oxide thickness of $t_{\mathrm{ox}} = 1.5\,\mathrm{nm}$, and random discrete dopants (RDD). To obtain the electrostatic potential self-consistently, we used the semi-classical 3D device simulator MinimosNT [11]. The simulator correctly treats random discrete dopants [12] and charged oxide defects. Quantum corrections are included by means of a density gradient (DG) model. For each nMOS device under investigation, we calculated the electrostatic potential once with the charged oxide defect and once without the defect.

Fig. 3 shows the current density calculated by the 2D NEGF model for a cut that goes through the charged defect. A significant reduction of the direct-tunneling current from the gate can be seen at the defect position. Furthermore, the gate leakage current flows straight through the oxide plane. This means that a 1D transport description is sufficient for our study of the direct-tunneling current.

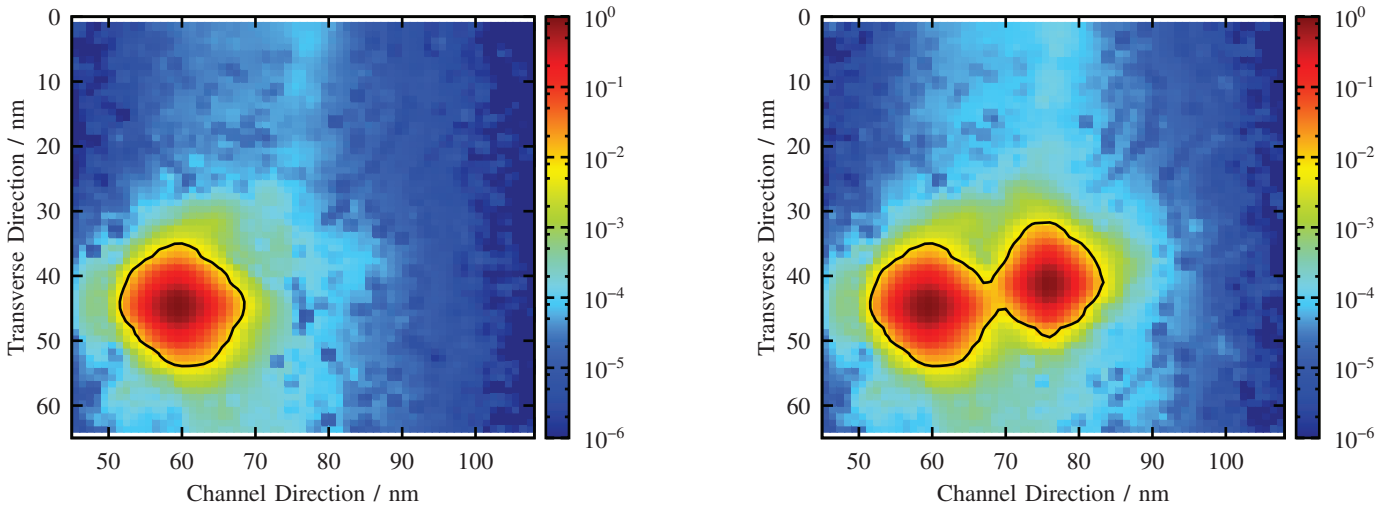

Fig. 5. Map of relative change in gate current density due to the charging of one trap (left) or two traps (right) for a particular doping and trap configuration. The map is constructed by a scan of 1D cuts over the whole gate area on a 1 nm grid. The plot shows high local changes in the current around the position of the trap. The contour line corresponds to 1 % of the maximum change in current. Its radius is below 10 nm and the current is therefore only locally influenced (cf. [3]). The total change is calculated by integration over the whole area. Contrary to the high local change around the trap, the total reduction in gate current is small ($\Delta I_{\mathrm{G}}/I_{\mathrm{G}} < 1\,\%$ per trap).

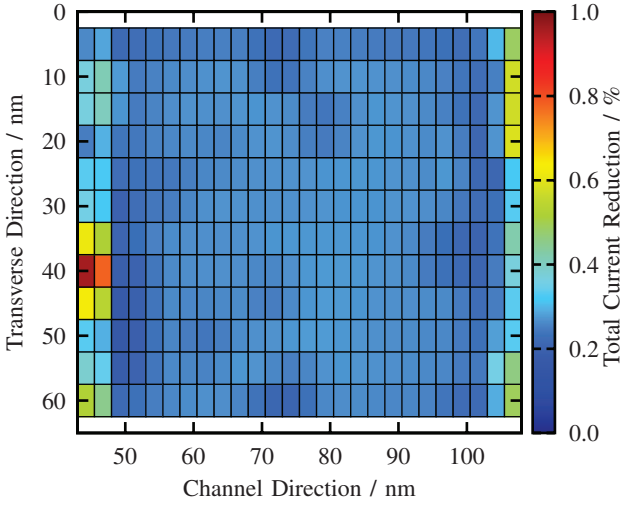

Fig. 6. Map of relative change in total gate current due to the charging of a trap at the given position for a particular doping configuration. Each box corresponds to a trap positioned at the center of the box and its color to the relative change of total gate current. A trap positioned close to the source or drain doping regions has a higher impact due to a higher field and more available carriers in these regions.

In Fig. 4 the local density of carriers on a cut through the defect position calculated by the 1D model illustrates the effect of the electrostatics on the carriers. The carriers are pushed away from the oxide decreasing the number of available electrons for direct tunneling and at the same time increasing the tunneling barrier.

To see the influence of one trap on the total gate leakage current, we employed a scan of 1D cuts over the whole gate area on a 1 nm grid. On each cut, we calculated the current density using the 1D NEGF model, once for the charged trap state and once for the empty trap state. Using these values we constructed a map of the relative change in current due to a trap (Fig. 5). The charged trap has a considerable local effect on the carriers and reduces the current density at its maximum by approximately 90 %. The extent of this change in direct tunneling can be estimated through the contour line in Fig. 5 were the change drops to 1 % of the maximum reduction. The radius of this contour is below 10 nm which is too small according to [3]. There, a uniformly influenced area of 25 nm radius was found to be necessary to explain the measurements.

We calculate the total gate leakage due to direct tunneling through integration over the whole gate area. Although the oxide defect has a considerable local impact, the total reduction in gate current due to charging of a single trap remains in the range $\Delta I_{\mathrm{G}}/I_{\mathrm{G}} < 1\,\%$.

To investigate the effect of the trap position on direct tunneling we mapped the relative change in total gate current (Fig. 6) depending on the defect's location. We moved a single trap on a grid along and across the channel and determined the total current reduction for each trap position. We found that a trap placed close to the source or drain doping regions has a higher impact. This is due to a higher field and more available carriers in these regions.

IV. Statistical Analysis

To study the effect of a charged trap on direct-tunneling gate leakage thoroughly, we performed a statistical analysis of $N_{\mathrm{S}} = 201$ nMOSFETs by varying the random discrete dopant configuration. The devices had an oxide thickness of $t_{\mathrm{ox}} = 1.5\,\mathrm{nm}$ and the gate voltage was $V_{\mathrm{G}} = 1\,\mathrm{V}$ to obtain sufficient direct-tunneling currents. We positioned a single electron trap near the drain region where direct tunneling is affected most, as confirmed by Fig. 6. We determined the 3D electrostatics for the charged and the inactive trap state using MinimosNT for each sample ($N_{\mathrm{T}} = 2$). We then calculated the direct-tunneling current density using the NEGF model on $N_{\mathrm{C}} = 64{\times}64 = 4{,}096$ 1D cuts per device and again integrated

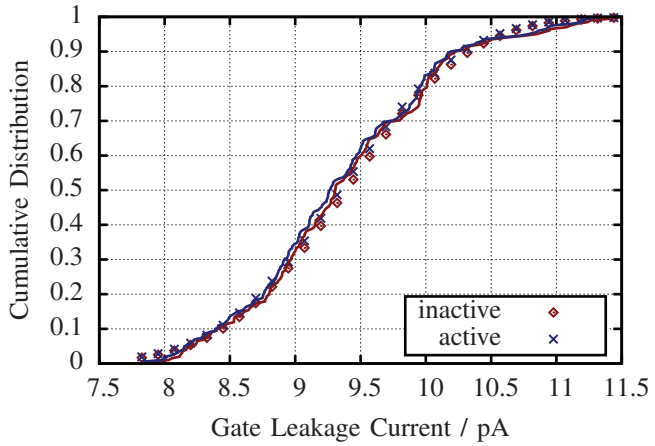

Fig. 7. Cumulative distribution of direct-tunneling gate currents with active (blue crosses) and inactive (red diamonds) trap. The symbols show the CDF of the fitted Gaussian distributions

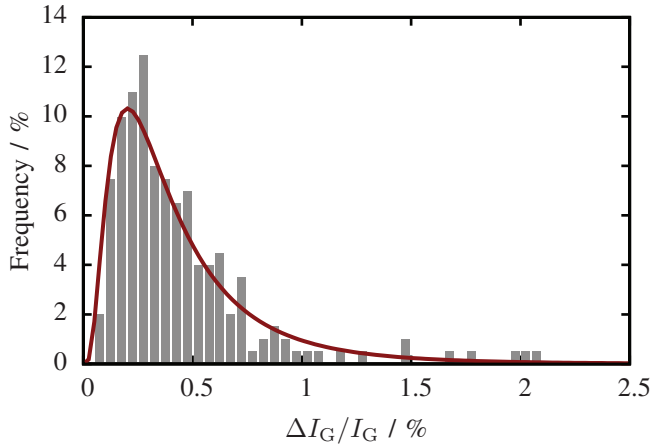

Fig. 8. Histogram of the relative differences of the direct-tunneling gate current with active and inactive trap showing a log-normal distribution (solid line). The mean reduction is $m \approx 0.45\,\%$ with a standard deviation of $0.38\,\%$

over the whole gate area to determine the total direct-tunneling current. Therefore, the total number of NEGF simulations was $N = N_S \times N_T \times N_C = 1{,}646{,}592$.

Fig. 7 shows the obtained cumulative distribution. The CDF for an active trap is shifted slightly to the left, due to the reduction in current. The relative change in direct-tunneling gate current $\Delta I_G/I_G$ is shown in Fig. 8. We also give the log-normal distribution for comparison to the histogram. It has a mean value of $m \approx 0.45\,\%$ and a standard deviation of about $0.38\,\%$. The experimental result of $\Delta I_G/I_G \approx 80\,\%$ can therefore not be explained by direct tunneling and alternative explanations such as the multi-state defect model for trap-assisted tunneling [5] must be sought.

V. Conclusion

We carried out a comprehensive study of correlated gate and drain current fluctuations in nMOS devices using non-equilibrium Green's function calculations. We investigated the effects of charged traps on the direct-tunneling current. Traps close to the source or drain region were found to have a higher impact on the tunneling current. We performed a statistical analysis of nMOSFETs with random discrete dopants and calculated the worst-case reduction in direct-tunneling current due to charging of a single trap. Our results show that electrostatic effects can not account for the large gate leakage fluctuations of up to $80\,\%$, that were found experimentally. Although a charged trap has a considerable influence on the local current density, the total gate leakage is reduced by less than $1\,\%$ per trap. Therefore, direct tunneling has to be ruled out as root cause of gate leakage fluctuations.

Acknowledgment

This work has been supported by the European Community's FP7 project n° 261868 (MORDRED) and the Austrian Science Fund, project I841-N24 (NAHDEVI). Global TCAD Solutions provided the GTS Framework for MinimosNT simulation setup and visualization [13].

References

[1] A. Asenov, A. Brown, J. Davies, S. Kaya, and G. Slavcheva, "Simulation of intrinsic parameter fluctuations in decananometer and nanometer-scale MOSFETs," *IEEE T. Electron. Dev.*, vol. 50, no. 9, pp. 1837–1852, 2003.

[2] M. Toledano Luque, B. Kaczer, E. Simoen, R. Degraeve, J. Franco, P. Roussel, T. Grasser, and G. Groeseneken, "Correlation of single trapping and detrapping effects in drain and gate currents of nanoscaled nFETs and pFETs," in *Proc. IRPS*, 4 2012, pp. XT.5.1 –XT.5.6.

[3] B. Kaczer, M. Toledano Luque, W. Goes, T. Grasser, and G. Groeseneken, "Gate current random telegraph noise and single defect conduction," *Microelectron. Eng.*, vol. 109, pp. 123–125, 2013, Insulating Films on Semiconductors 2013. [Online]. Available: http://www.sciencedirect.com/science/article/pii/S0167931713003390

[4] C.-Y. Chen, Q. Ran, H.-J. Cho, A. Kerber, Y. Liu, M.-R. Lin, and R. Dutton, "Correlation of Id- and Ig-random telegraph noise to positive bias temperature instability in scaled high-k/metal gate n-type MOSFETs," in *Proc. IRPS*, 2011, pp. 3A.2.1–3A.2.6.

[5] T. Grasser, H. Reisinger, P. J. Wagner, F. Schanovsky, W. Goes, and B. Kaczer, "The time dependent defect spectroscopy (TDDS) for the characterization of the bias temperature instability," in *Proc. IRPS*, 5 2010, pp. 16–25.

[6] M. Karner, A. Gehring, S. Holzer, M. Pourfath, M. Wagner, W. Goes, M. Vasicek, O. Baumgartner, C. Kernstock, K. Schnass, G. Zeiler, T. Grasser, H. Kosina, and S. Selberherr, "A Multi-Purpose Schrödinger-Poisson Solver for TCAD Applications," *J. Comput. Electron.*, vol. 6, no. 1, pp. 179–182, 9 2007. [Online]. Available: http://dx.doi.org/10.1007/s10825-006-0077-7

[7] O. Baumgartner, M. Karner, S. Holzer, M. Pourfath, T. Grasser, and H. Kosina, "Adaptive Energy Integration of Non-Equilibrium Green's Functions," in *Proc. NSTI Nanotech*, vol. 3, 2007, pp. 145–148.

[8] O. Baumgartner, M. Karner, and H. Kosina, "Modeling of High-k-Metal-Gate-Stacks Using the Non-Equilibrium Green's Function Formalism," in *Proc. SISPAD*, 9 2008, pp. 353–356.

[9] R. Lake, G. Klimeck, R. C. Bowen, and D. Jovanovic, "Single and Multiband Modeling of Quantum Electron Transport through Layered Semiconductor Devices," *J. Appl. Phys.*, vol. 81, no. 12, pp. 7845–7869, 6 1997.

[10] A. Svizhenko, M. P. Anantram, T. R. Govindan, B. Biegel, and R. Venugopal, "Two-Dimensional Quantum Mechanical Modeling of Nanotransistors," *J. Appl. Phys.*, vol. 91, no. 4, pp. 2343–2354, 2 2002.

[11] M. Bina, O. Triebl, B. Schwarz, M. Karner, B. Kaczer, and T. Grasser, "Simulation of Reliability on Nanoscale Devices," in *Proc. SISPAD*, 2012, pp. 109–112.

[12] A. Asenov, "Random dopant induced threshold voltage lowering and fluctuations in sub-0.1 µm MOSFET's: A 3-D "atomistic" simulation study," *IEEE T. Electron. Dev.*, vol. 45, no. 12, pp. 2505–2513, 1998.

[13] "GTS Framework," [Online; accessed 2013-07-02]. [Online]. Available: http://www.globaltcad.com/en/products/gts-framework.html